Indian Journal of Chemistry
Vol. 60A, January 2021, pp. 51-61

Computational structure characterization, nonlinear optical properties and antitumor activities of Nickel(II) complexes containing alkoxy-derived dicyandiamide ligands

Tuba Alagöz Sayın & Duran Karakaş*

Sivas Cumhuriyet University, Science Faculty, Chemistry Department, 58140 Sivas, Turkey

*E-mail: dkarakas@cumhuriyet.edu.tr

Received 18 June 2020; revised and accepted 05 October 2020

$[Ni(dcda\text{-}O\text{-}Me)_2]^{2+}$ **(1)**, $[Ni(dcda\text{-}O\text{-}Et)_2]^{2+}$ **(2)**, $[Ni(dcda\text{-}O\text{-}nPr)_2]^{2+}$ **(3)**, and $[Ni(dcda\text{-}O\text{-}nBu)_2]^{2+}$ **(4)** complexes (dcda-O-R is dicyandiamide ligands with alkoxy-derived) have been optimized in the gas phase at B3LYP/LANL2DZ/6-31+G(d,p) level. Computational structure characterization has been performed from the structural parameters, IR spectra, ^{1}H-NMR, ^{13}C-NMR chemical shift values. It has been found that the central metal atom geometry in the complexes is a distorted square plane. Some electronic structure descriptors of the complexes are calculated in the gas phase and nonlinear optical properties are predicted. Complex **1** is found as the most suitable compound to produce optical material. The complexes are optimized at the same level in the aqueous phase to determine antitumor activity. Some electronic structure descriptors are calculated and molecular docking calculations are made against the 3WZE protein. According to the calculated electronic structure descriptors and molecular docking results, it is found that the complex **3** has the highest antitumor activity against the selected target protein.

Keywords: Dicyandiamide, Ni(II) complexes, Computational structure characterization, NLO properties, Antitumor activity

Dicyandiamide (dcda) is a ligand having two tautomeric structures as N≡C–N=C$(NH_2)_2$ and N≡C-NHC(=NH)NH_2. As seen from tautomeric structures, the dcda ligand contains a nitrile group (N≡C-). Nitrile is an active group and forms dicyandiamide derivatives by giving nucleophilic addition reactions with water, alcohols, and amines in the presence of transition metal ions. While guanylurea is formed by the nucleophilic addition of water to dicyandiamide, 1-amidino-O-alkylurea is formed by the nucleophilic addition of alcohols, and biguanides are formed from the nucleophilic addition of amines[1-5]. There is no significant reaction between dicyandiamide and alcohols when there is no metal ion. However, the addition of alcohol to dicyandiamine in the presence of the Cu(II) ion results in high yields, while the same reaction takes a long time in the presence of Ni(II), requires a base, and the yield is low[6,7].

Dicyandiamide and its derivatives form complexes with transition metals. Transition metal complexes have widespread use due to their biological, catalytic, and optical properties. Because of their catalytic properties, they are used as catalysts in many industrial processes such as alkene polymerization[8], olefin metathesis[9], and Wacker process[10]. Due to their biological activities, they are used as antimicrobial, antibacterial, antibiotic, antitumor drugs in the health field[11-16]. Due to their optical properties, they are used in the production of valuable optical materials such as optical modulation, optical switching, optical logic, and optical memory[17,18]. The biological, catalytic, and optical properties of transition metal complexes depend on many factors such as the type of metal, the oxidation state of the metal, the type of ligand, the number of donor atoms of the ligand and the coordination number of the complex. The change in each of these factors gives the complex a different feature and complex activity changes.

The syntheses and molecular structure determination of $[Ni(dcda\text{-}O\text{-}R)_2]^{2+}$ type four-coordinated complexes were reported by Kose et al. Also, it has been experimentally found that complexes have higher antimicrobial activity than ligands against some microorganisms[19]. However, there is no study on nonlinear optical (NLO) properties and antitumor activity of the complexes.

In this study, we aimed to determine the molecular structures of the complexes {$[Ni(dcda\text{-}O\text{-}Me)_2]^{2+}$ **(1)**, $[Ni(dcda\text{-}O\text{-}Et)_2]^{2+}$ **(2)**, $[Ni(dcda\text{-}O\text{-}^{n}Pr)_2]^{2+}$ **(3),** and $[Ni(dcda\text{-}O\text{-}^{n}Bu)_2]^{2+}$ **(4)**} by quantum chemical

intensity. Therefore, their peaks are not taken into account. The vibrations forming the peaks given in Fig. 2 and the frequencies of the peaks are presented in Table 2. Experimental values are taken from reference[18].

The frequencies calculated in Table 2 are harmonic and the experimental frequencies are anharmonic. To obtain anharmonic frequencies from harmonic frequencies, there must be a scale factor at each calculation level. However, there is no scale factor for B3LYP/LANL2DZ/6-31+G(d,p) level in the literature. When the frequency scale factors in the literature for various levels are examined, it is seen that it varies in the range of 0.89-1.0[24]. If the harmonic frequencies in Table 2 are multiplied by a number in the range 0.89-1.0, it is seen to be quite compatible with the experimental values.

As seen in Table 2, the peaks characteristic for the complexes belong to the Ni-N, R-O, C-N, C=N, C-H, and N-H stretching vibrations. As expected, the Ni-N peak was found at low frequency and the N-H peak at the highest frequency. The fact that the force constant of the Ni-N bond is small and its reduced mass is large causes it to be observed at a lower frequency. This finding is compatible with the literature[34]. Because metal-ligand bond stretching vibrations are often observed at low frequencies. The peaks of the C-N stretching vibrations in the complexes were calculated at about 1570 cm^{-1} and the peaks of the C=N vibrations at about 1715 cm^{-1}. This finding is consistent with the bond force constant. Because the reduced masses of C-N and C=N are the same, only the bond force constants are different. Since the C=N bond force constant is greater than that of C-N, it was observed at high frequency. The frequencies of the R-O stretching vibrations fall into the single bond stretching region. R-O stretching vibrations for the complexes were observed in the range of 868-953 cm^{-1}.

NMR chemical shift values

One of the most preferred techniques in molecular structure characterization is NMR spectroscopy. By NMR spectroscopy, ^{13}C, and ^{1}H-NMR spectra of molecules can be obtained and chemical shift values can be calculated. Chemical shifts can be used to determine the equivalent atoms in molecules and to predict the molecular structure. ^{13}C-NMR and ^{1}H-NMR spectra of the complexes examined in this study were calculated in the gas phase using the GIAO method at the level of B3LYP/LANL2DZ/6-31+G(d,p). In the interpretation of NMR spectra, tetramethylsilane (TMS) was taken as a reference. TMS was optimized at B3LYP/6-31+G(d,p) level. Shielding of carbon and hydrogen atoms in TMS was obtained as 192.5 and 31.6 ppm by using GIAO method in the gas phase. Chemical shifts of ^{13}C-NMR

Table 2 — Vibrations that form high-intensity peaks and the frequencies (cm^{-1}) of the peaks calculated at B3LYP/LANL2DZ/6-31+G(d,p) level

		Complex (1)		Complex (2)	
Peak	Vibrations	Calc.	Exp.	Calc.	Exp.
1	δ_{oop}(N-H)	687.5	-	686.8	-
2	ν_{as}(Ni-N)	744.7	556	742.8	553
3	ν_{as}(R-O)	952.3	-	868.8	-
4	δ_{ip}(N-H) + ν_{s}(C-O)	1260.9	-	1256.5	-
5	ν_{as}(C-N)	1570.9	-	1571.5	-
6	ν_{as}(C=N)	1718.4	1655	1716.2	1655
7	ν_{s}(N-H+NH_2)	3605.9	3366	3609.7	3346
8	ν_{as}(NH_2)	3713.5	3455	3715.9	3446
		Complex (3)		Complex (4)	
Peak	Vibrations	Calc.	Exp.	Calc.	Exp.
1	δ_{oop}(N-H)	686.8	-	687.2	-
2	ν_{as}(Ni-N)	744.8	556	745.2	564
3	ν_{as}(R-O)	928.3	-	927.8	-
4	δ_{ip}(N-H) + ν_{s}(C-O)	1256.4	-	1256.3	-
5	ν_{as}(C-N)	1569.2	-	1569.3	-
6	ν_{as}(C=N)	1715.8	1655	1715.6	1662
7	ν(C-H)	3127.6	2977	3121.0	2941
8	ν_{s}(N-H+NH_2)	3609.2	3345	3609.4	3343
9	ν_{as}(NH_2)	3716.5	3456	3716.8	3441

ν_{as}: Asymmetric stretching, ν_{s}: Symmetric stretching, δ_{oop}: Out of plane deformation, δ_{i}: In-plane deformation, R: Alkyl group

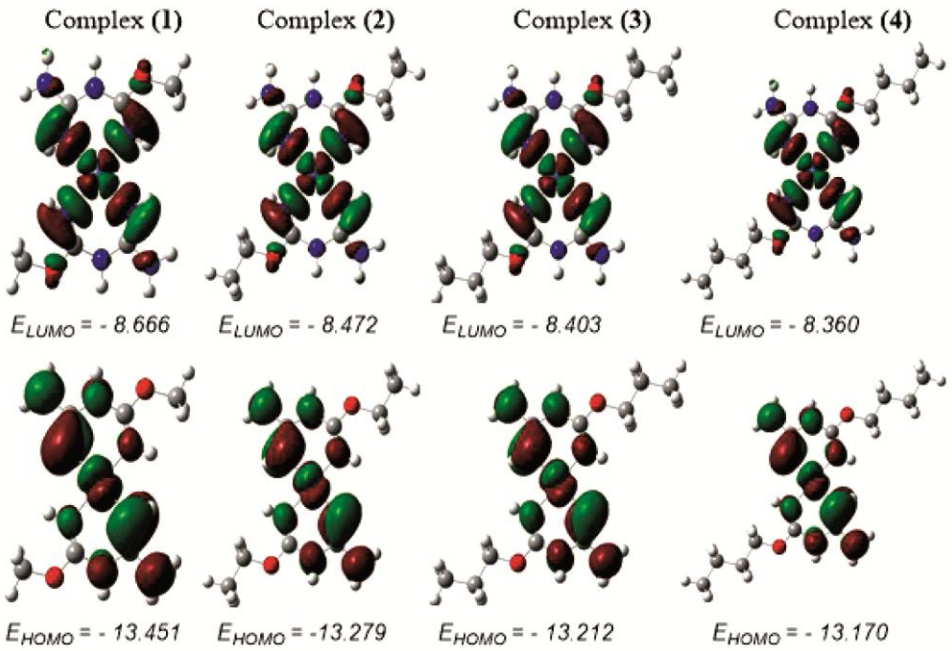

Fig. 3 — HOMO and LUMO contour diagrams and energies of the studied complexes

Table 4 — Calculated electronic structure descriptors for complex (1) – (4) and urea in the gas phase

Descriptor	Complex (1)	Complex (2)	Complex (3)	Complex (4)	Urea
E_{LUMO}[1]	-8.666	-8.472	-8.403	-8.360	-0.373
E_{HOMO}[1]	-13.451	-13.279	-13.212	-13.170	-7.318
I[1]	13.451	13.279	13.212	13.170	7.318
A[1]	8.666	8.472	8.403	8.360	0.373
ΔE[1]	4.785	4.806	4.809	4.810	6.944
η[1]	2.392	2.403	2.404	2.405	3.472
σ[2]	0.418	0.416	0.416	0.416	0.288
S[2]	0.209	0.208	0.208	0.208	0.144
χ[1]	11.059	10.876	10.807	10.765	3.846
μ_{cp}[1]	-11.059	-10.876	-10.807	-10.765	-3.846
ω[1]	25.558	24.608	24.288	24.091	2.130
ε[2]	0.039	0.041	0.041	0.042	0.470
α[3]	159.389	186.135	211.273	237.264	32.735
μ[4]	$2.2x10^{-4}$	$2.2x10^{-4}$	$11.2x10^{-4}$	$3.0x10^{-4}$	4.566

[1]eV, [2]eV^{-1}, [3]a.u, [4]Debye,

HOMO and LUMO energies increase from the complex (1) to complex (4). Some electronic structure descriptors such as ionization energy (I), electron affinity (A), energy gap (ΔE), hardness (η), softness (σ), global softness (S), absolute electronegativity (χ), chemical potential (μ_{cp}), electrophilicity index (ω), nucleophilicity index (ε), average molecular polarizability (α), and static dipole moment (μ) were calculated in the gas phase using frontier molecular orbital energies for the complexes and reference urea and given in Table 4.

Ionization energy and electron affinity values are equal to the opposite sign of HOMO and LUMO energies according to the Koopmans theorem[35]. The ionization energy of molecules shows the tendency to give electrons, and the electron affinity indicates the tendency to receive. In molecules with high ionization energy and electron affinity, electrons are more attracted by nuclei and electron mobility and NLO feature decrease.

A smaller energy gap indicates that charge transfer within the molecule is easier and the NLO property is

Table 6 — Some electronic structure descriptors for complex (1)-(4) and cisplatin calculated at B3LYP/LANL2DZ/6-31+G(d,p) level in the aqueous phase

Descriptor	Complex (1)	Complex (2)	Complex (3)	Complex (4)	Cisplatin
E_{LUMO}[1]	-2.479	-2.465	-2.454	-2.464	-1.932
E_{HOMO}[1]	-7.251	-7.218	-7.238	-7.197	-6.604
I[1]	7.251	7.218	7.238	7.197	6.604
A[1]	2.479	2.465	2.454	2.464	1.932
ΔE[1]	4.772	4.753	4.784	4.733	4.672
η[1]	2.386	2.376	2.392	2.366	2.336
σ[2]	0.419	0.421	0.418	0.423	0.428
S[2]	0.209	0.210	0.209	0.211	0.214
χ[1]	4.865	4.841	4.846	4.830	4.268
μ_{cp}[1]	-4.865	-4.841	-4.846	-4.830	-4.268
ω[1]	4.960	4.931	4.909	4.929	3.899
ε[2]	0.202	0.203	0.204	0.203	0.256
α[3]	205.1	236.5	267.8	297.8	116.9

[1]eV, [2]eV^{-1}, [3]a.u.

Table 7 — Antitumor activity ranking for complex (1) - (4) and cisplatin according to **c**alculated electronic structure descriptors

Descriptor	Antitumor activity ranking
I, χ, μ_{cp}	cisplatin > Complex (4) > Complex (2) > Complex (3) > Complex (1)
A, ω, ε	cisplatin > Complex (3) > Complex (4) > Complex (2) > Complex (1)
ΔE, η, σ	cisplatin > Complex (4) > Complex (2) > Complex (1) > Complex (3)
S	cisplatin > Complex (4) > Complex (2) > Complex (1) = Complex (3)
α	Complex (4) > Complex (3) > Complex (2) > Complex (1) > cis-platin

Except for the average molecular polarizability order, the rankings in Table 7 show that the antitumor activity of the complexes is lower than cisplatin. These results do not mean that the complexes have no antitumor activity. According to the quantitative structure-activity relationship (QSAR) model, electronic structure descriptors do not contribute equally to antitumor activity[37]. That is, the antitumor activity can only result from average molecular polarizability.

Molecular docking studies

Molecular docking is the process of finding the best match and interaction between two molecules. The best interaction is represented by binding energy. Binding energy includes interactions such as van der Waals interactions, electrostatic interactions, hydrogen bonds, hydrophobic interactions. The magnitude of the binding energy is a measure of the stability of the ligand-receptor complex.

Previous studies show that inhibition of vascular endothelial growth factor receptor-2 (VEGFR-2) is one of the anticancer mechanisms[38]. Therefore, VEGFR-2 was chosen as the target protein in this study. The protein data bank (PDB) code of VEGFR-2 is 3WZE. Molecular docking calculations were made between complex (**1**) – (**4**) and 3WZE cell lines. Hex 8.0.0 docking program was used in calculations. Docking poses of the complex (**1**) – (**4**) against 3WZE cell lines are given in Fig. 4.

As seen in Fig. 4, complexes almost interacted with the same region in the 3WZE protein. This zone, where complexes enter, is the active zone of 3WZE cells. Binding energy is maximum in this region. Binding energies for complex (**1**), complex (**2**), complex (**3**), and complex (**4**) were calculated as -262.1, -295.9, -329.7, and -309.0 kcal/mol, respectively. Reference cisplatin was also docked against the same cell line under the same conditions. The binding energy between cisplatin and 3WZE cell lines was calculated as -258.4 kcal/mol. These results show that the binding energy between the complex **(1)** – **(4)** and 3WZE cell lines is greater than that of the cisplatin. Therefore, complex **(1)-(4)** can be considered as an anticancer drug candidate. The anticancer activity ranking of the complexes examined according to the binding energies against the 3WZE cell lines is as follows:

Cisplatin< Complex (**1**)< Complex (**2**)< Complex (**4**)< Complex (**3**).

According to these findings, it can be said that complex (**3**) is the most suitable drug candidate for VEGFR-2.